

# Modeling of Magnetic Hysteresis

Seiji Hayano and Yoshifuru Saito (Hosei University)

## Abstract

This paper reviews the classical magnetization models for computational use. for the magnetodynamics in ferromagnetic materials. At first, Fourier model of the hysteretic magnetization is derived. Second, assuming the bar-like domain walls derives a domain-based model. A simple example verifies this validity of domain-based model. Third, a composite model by combining the Preisach with domain-based models is derived.

Key words : Magnetism, Hysteresis, Modeling

## 1. Introduction

Modeling of the ferromagnetic materials is of paramount importance for modern computational magneto-dynamics in order to carry out the practical magnetic device design. Fundamentally, the elements comprising the modern electronic as well as electrical devices are classified into two major categories. One is the active element such as silicon controlled rectifier and Power MOS FET. The other is the passive element such as resistance, capacitance and inductance. Even if the inductors are regarded as one of the linear elements in the undergraduate textbook, practically most of them exhibit a serious non-linearity, e.g., saturation and hysteretic properties.

In the present paper, at first, we derive a phenomenological magnetization model by means of Fourier series. Second,

assuming the bar-like domain walls leads to a domain-based model. Third, a composite model by combining the Preisach with domain-based models is derived. Analytical solution of this composite model leads to the famous Lord Rayleigh's law.

Thus, this paper suggests an implementation methodology of computer-aided magnetic device design fully taking into account the magnetization characteristics in ferromagnetic materials.

## 2. Modeling of Ferromagnetic Magnetization

### 2.1 Model by Fourier series

Consider the sinusoidal time  $t$  varying flux densities  $B$  having angular frequency  $\omega$ ,

$$B = B_m \sin(\omega t), \quad (1)$$

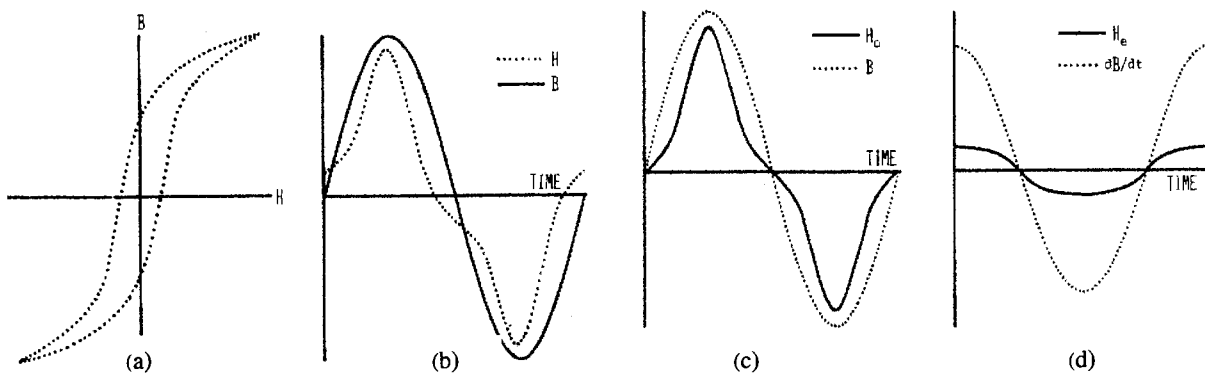


Fig.1. Typical hysteresis loop and in phase components in time.

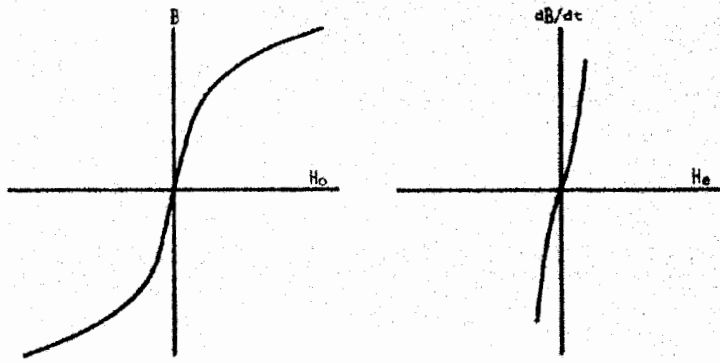


Fig.2.  $B$  vs  $H_o$  (Left) and  $dB/dt$  vs  $H_e$  (Right)

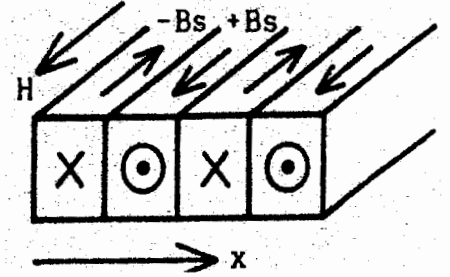


Fig.3. Bar-like magnetic domains

then, as shown in Figs.1(a) and 1(b), we have the distorted field intensities  $H$  in (2) represented in terms of Fourier series.

$$\begin{aligned} \mathbf{H} &= \sum_{n=1}^{\infty} \mathbf{H}_n \sin(n\omega t) + \sum_{n=1}^{\infty} \mathbf{H}_n \cos(n\omega t) \\ &= \mathbf{H}_o + \mathbf{H}_e, \end{aligned} \quad (2)$$

where  $H_o$  and  $H_e$  are the odd and even components of the distorted field  $H$ , respectively.

As shown in Figs. 1(c) and (d), the odd component  $H_o$  and even component  $H_e$  are, respectively, in phase with the flux density  $B$  and the time derivative  $dB/dt$ . Thereby, a combination of  $H_o$  with  $B$  yields one of the saturation curves. Also, a combination of  $H_e$  with  $dB/dt$  yields a curve which represents the hysteretic property, because  $H_e(dB/dt)$  provides the power loss per unit volume. Figs. 2(Left) and (Right) show the  $B$  vs.  $H_o$  and  $dB/dt$  vs.  $H_e$  curves, respectively. In the other words, by considering the relationship of Figs. 2(a) and (b), it is possible to derive a following Fourier based magnetization model (3).

$$\mathbf{H} = \mathbf{H}_o + \mathbf{H}_e = \frac{1}{\mu} \mathbf{B} + \frac{1}{s} \frac{d\mathbf{B}}{dt}, \quad (3)$$

where  $\mu, s$  are the permeability and hysteresis coefficient, respectively [1].

## 2.2 Domain-based Model

To derive a constitutive equation representing magnetization characteristics of ferromagnetic materials, let us consider a simple bar-like domain wall model shown in Fig.3. When an external magnetic field  $\mathbf{H}_s$  is applied, (4) can be established.

$$\begin{aligned} \mathbf{B} &= \mu_0 \mathbf{H}_s + n\mathbf{B}_s \\ &= \mu_0 \left(1 + \mathbf{H}_s^{-1} \mathbf{B}_s\right) \mathbf{H}_s = \mu \mathbf{H}_s \end{aligned} \quad (4)$$

where  $\mathbf{B}_s, n, \mu_0$  and  $\mu$  are the saturation flux density in each of

the domains, number of domains in accordance with the direction of  $\mathbf{H}_s$ , permeability of air, and permeability of the specimen, respectively. The constitutive equation should exhibit various magnetization characteristics, such as a hysteretic property. This means that the constitutive equation must be composed of parameters not affected by past histories. One of the unique properties independent of the past histories is an ideal or anhysteretic magnetization curve. If (4) has been established for the ideal magnetization curve, then obviously (4) represents a static magnetization characteristic corresponding to each of the domain situations. This means that the permeability  $\mu$  in (4) can be obtained from the ideal magnetization curve.

Differentiation (4) with time  $t$  yields a following relation:

$$\begin{aligned} \frac{d\mathbf{B}}{dt} &= \mu_0 \frac{d\mathbf{H}}{dt} + \mathbf{B}_s \frac{dn}{dt} \\ &= \left( \mu_0 + \mathbf{B}_s \frac{\partial n}{\partial \mathbf{H}} \right) \frac{d\mathbf{H}}{dt} + \mathbf{B}_s \frac{\partial n}{\partial x} \frac{dx}{dt} \\ &= \mu_r \frac{d\mathbf{H}}{dt} + \mathbf{B}_s \frac{\partial n}{\partial x} v, \end{aligned} \quad (5)$$

where  $\mathbf{H}, v$ , and  $\mu_r$  are the applied field, velocity ( $dx/dt$ ) of domain movement, and reversible permeability, respectively. Consideration of (5) suggests that the induced voltage per unit area ( $dB/dt$ ) is composed of the transformer and velocity induced

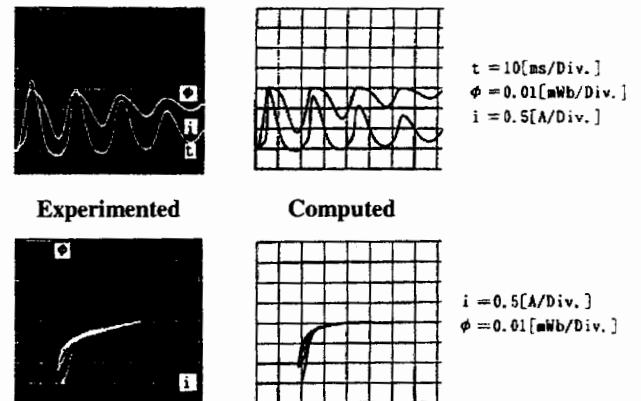


Fig.4. Experimented and computed results (K6A, TDK).

voltages. When a hysteresis coefficient  $s$  ( $\Omega/m$ ) is introduced into (5), the magnetic field  $H_d$  due to the domain movement is given by

$$H_d = \frac{1}{s} B_s \frac{\partial n}{\partial x} v = \frac{1}{s} \left( \frac{dB}{dt} - \mu_r \frac{dH}{dt} \right), \quad (6)$$

where it has been assumed that the width of the domains is fixed and only their number changes as the specimen magnetized. Summation of the static field  $H_s$  in (4) and dynamic field  $H_d$  in (6) gives the domain-based magnetization model as [2]

$$\begin{aligned} H &= H_s + H_d = \frac{1}{\mu} B + \frac{1}{s} B_s \frac{\partial n}{\partial x} v \\ &= \frac{1}{\mu} B + \frac{1}{s} \left( \frac{dB}{dt} - \mu_r \frac{dH}{dt} \right). \end{aligned} \quad (7)$$

We had carried out intensive experimental verification of (7). Fig.4 shows one of the examples.

### 2.3 Preisach and Composite Models

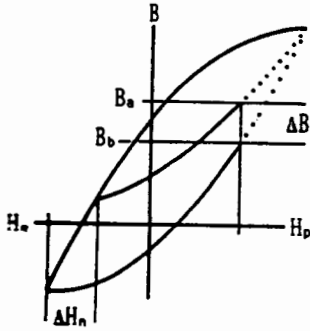


Fig.5. Derivation of Preisach model.

According to Ref. [3], a reversing  $H_n$  and applied  $H_p$  field points are defined as shown in Fig. 5. By considering the trajectories in Fig.5, it is obvious that  $B$ - $H$  trajectory takes different paths depending on the reversing field  $H_n$ . Thereby, the flux density  $B$  is represented as a function of applied field  $H_p$  as well as reversing field  $H_n$ :

$$B = f(H_p, H_n). \quad (8)$$

Moreover, consideration of a saturation flux density suggests that the  $B$ - $H$  trajectories take different paths depending on the reversing fields  $H_n$ , but always coincide at the saturation flux density. Thereby, rate of change  $\partial B / \partial H_p$  with reversing field  $H_n$  takes non-zero value within the unsaturated region. This leads to the definition of the Preisach function  $\Psi$  as

$$\Psi = \frac{\partial^2 B}{\partial H_n \partial H_p}. \quad (9)$$

Application (5) to the magnetizing states shown in Fig. 5 gives

$$H_p = \frac{1}{\mu} B_a + \frac{1}{s} \left( \frac{\partial B_a}{\partial t} - \mu_r \frac{\partial H_p}{\partial t} \right), \quad (10)$$

$$H_p = \frac{1}{\mu} B_b + \frac{1}{s} \left( \frac{\partial B_b}{\partial t} - \mu_r \frac{\partial H_p}{\partial t} \right), \quad (11)$$

where the field  $\Delta H_n$  in Fig. 5 is so small that the parameters  $\mu$ ,  $\mu_r$ ,  $s$  are assumed to be constants.

Subtracting (11) from (10) yields

$$\begin{aligned} \frac{\Delta B}{\mu} &= \frac{B_a - B_b}{\mu} = \frac{1}{s} \left( \frac{\partial B_a}{\partial t} - \frac{\partial B_b}{\partial t} \right) \\ &= \frac{1}{s} \left( \frac{\partial B_a}{\partial H_p} - \frac{\partial B_b}{\partial H_p} \right) \frac{\partial H_p}{\partial t}. \end{aligned} \quad (12)$$

Rearrangement of (12) gives

$$\frac{s}{\partial H_p / \partial t} = \frac{\mu}{\Delta B} \left( \frac{\partial B_b}{\partial H_p} - \frac{\partial B_a}{\partial H_p} \right). \quad (13)$$

In Fig. 5, if the limit of  $\Delta H_n$  goes to zero, then  $\Delta B / \mu$  is simultaneously to be zero. Thus, an assumption  $\Delta H_n = \Delta B / \mu$  leads to

$$\lim_{\Delta H_n \rightarrow 0} \frac{\mu}{\Delta B} \left( \frac{\partial B_b}{\partial H_p} - \frac{\partial B_a}{\partial H_p} \right) = \frac{\partial^2 B}{\partial H_n \partial H_p}. \quad (14)$$

From (9), (13) and (14), the hysteresis coefficient  $s$  in (6) is related to the Preisach function  $\Psi$  by

$$s = \Psi \frac{\partial H}{\partial t}. \quad (15)$$

Substituting (15) into (7) after some modification (7) yields a following composite model:

$$H + \frac{\mu_r}{\Psi} = \frac{1}{\mu} B + \frac{1}{\Psi} \frac{dB}{dt}. \quad (16)$$

Let us consider that the parameters  $\mu$ ,  $\mu_r$ ,  $\Psi$  take the constants in the weakly magnetized region known as the Rayleigh region, then (16) gives

$$\begin{aligned} B &= \mu (H_n + H_p) \\ &+ \frac{\mu^2}{\Psi} \left( 1 - \frac{\mu_r}{\mu} \right) \left( \varepsilon^{-\frac{\mu}{\Psi}(H_n + H_p)} - 1 \right) - B_n \varepsilon^{-\frac{\mu}{\Psi}(H_n + H_p)}. \end{aligned} \quad (17)$$

where  $H_p$ ,  $H_n$  and  $B_n$  are the applied and reversing point fields and reversing point flux density, respectively. The fields  $H_p$  and  $H_n$  are so small that the following approximations could be held:

$$\varepsilon^{-\frac{\mu}{\psi}(\mathbf{H}_p + \mathbf{H}_n)} \approx 1 - \frac{\mu}{\psi}(\mathbf{H}_p + \mathbf{H}_n) + \frac{1}{2} \left[ \frac{\mu}{\psi}(\mathbf{H}_p + \mathbf{H}_n) \right]^2. \quad (18)$$

Substituting (18) into (17) and setting  $\mathbf{H}_n = \mathbf{B}_n = 0$  yields

$$\mathbf{B} = \mu_r \mathbf{H}_p + \frac{1}{2} \psi \mathbf{H}_p^2 \left( 1 - \frac{\mu_r}{\mu} \right) \approx \mu_r \mathbf{H}_p + \frac{1}{2} \psi \mathbf{H}_p^2, \quad (19)$$

where  $\mu \gg \mu_r$  has been assumed. (19) is obviously Rayleigh's initial magnetization curve [3]. Hence, it is revealed that the Preisach function  $\Psi$  corresponds to the Rayleigh's constant. Imposing symmetrical  $\mathbf{B}$ - $\mathbf{H}$  loop condition to (16) yields the reversing flux density  $\mathbf{B}_n$  as

$$\mathbf{B}_n = \mu \mathbf{H}_n + \left( \mu \mathbf{H}_n - \frac{\mu^2}{\psi} + \frac{\mu_r \mu}{\psi} \right) \tanh \left( \frac{\psi}{\mu} \mathbf{H}_n \right) \quad (20)$$

After employing the approximations as these of the derivation (19), substituting this into (20) yield a lower branch of Rayleigh loop:

$$\mathbf{B} = (\mu_r + \psi \mathbf{H}_n) \mathbf{H}_p + \frac{1}{2} (\mathbf{H}_p^2 - \mathbf{H}_n^2). \quad (21)$$

Thus, the composite model (16) is including all of the Rayleigh's Law.

### 3. Conclusion

As shown above, we have derived the magnetization model by means of Fourier series. Assuming the bar-like domain walls has lead to a domain-based model. Finally, a composite model by combining the Preisach with domain-based models has been derived. Analytical solution of this composite model leads to the Rayleigh's law.

### References

- [1] Y.Saito, S.Hayano, H.Nakamura, Y.Kishino and N.Tsuya, A Representation of Magnetic Hysteresis by Fourier Series. *Journal of Magnetic Materials* 54-57, 1986, pp.1613-1614.
- [2] S.Hayano, M.Namiki and Y.Saito, A Magnetization Model for Computational Magnetodynamics, *JAP*, 69(8), 15 April 1991, pp.4641-4616.
- [3] Y.Saito, K.Fukushima, S.Hayano and N.Tsuya, Application of a Chua Type Model to the Loss and Skin Effect Calculations, *IEEE Trans. Magnetics.*, Vol. MAG-23, No. 5, September 1987, pp.2227-2229.

原稿受付日

平成 15 年 3 月 4 日